SCIENCE CHINA
Chemistry

• FEATURE ARTICLES •

February 2010 Vol.53 No.2: 365–371
doi: 10.1007/s11426-010-0041-z

Solution-phase synthesis of inorganic nanostructures by chemical transformation from reactive templates

HUANG Teng & QI LiMin*

Beijing National Laboratory for Molecular Sciences (BNLMS), State Key Laboratory for Structural Chemistry of Unstable and Stable Species, College of Chemistry, Peking University, Beijing 100871, China

Received August 30, 2009; accepted November 11, 2009

The solution-phase synthesis by chemical transformation from reactive templates has proved to be very effective in morphology-controlled synthesis of inorganic nanostructures. This review paper summarizes the recent progress in solution-phase synthesis of one-dimensional and hollow inorganic nanostructures via reactive templates, focusing on the approaches developed in our lab. The formation mechanisms based on reactive templates are discussed in depth to show the general concepts for the preparation processes. An outlook on the future development in this area is also presented.

reactive template, morphology-controlled synthesis, nanostructures, one-dimensional structures, hollow structures

1 Introduction

One-dimensional (1D) nanostructures such as wires, rods, belts and tubes have stimulated intensive interest because they provide an ideal system for investigations on the dimensionality and size dependence of the electrical and optical properties of nanomaterials, and they are expected to be utilized as both interconnects and functional units in fabricating electronic, optoelectronic, electrochemical, and electromechanical devices with nanoscale dimensions [1–3]. On the other hand, hollow micro-/nanostructures have received considerable attention because of their advantageous properties including high surface area, low density, and large fraction of void space as well as potential applications in controlled drug delivery, catalysis, sensors, lightweight fillers, low-dielectric-constant thin films, photonic crystals, confined-space chemical reactors, biomedical diagnosis and therapy [4–6]. Hence the controlled synthesis of these inorganic nanostructures has been extensively studied [1, 4, 7, 8].

The template method is an effective approach for the controlled synthesis of nanomaterials with both 1D and hollow morphologies [8–11]. Hard templates such as polymer or anodic aluminum oxide (AAO) membranes [10], mesoporous silica [12], and Sephadex gel beads [13] as well as soft templates including surfactants [14–16], polymers [17–20], surfactant–polymer mixtures [21–23], DNA and peptide chains [24, 25], and emulsion droplets [26] have been widely used for this purpose. However, harsh conditions or complicated procedures are generally required to remove hard templates, and the templating effects are not so straightforward in many cases for soft templates. Reactive templates, which act as both templates and reactive precursors or intermediates, are not only free from the template removal problem but also free from the limited morphologies of hard templates, because the precursors can be fabricated through all the techniques developed for morphosynthesis of nanomaterials [4, 7, 8, 11]. In this regard, a variety of 1D and hollow inorganic nanostructures have been successfully prepared by employing reactive sacrificial templates [27–30]. This feature article summarizes our recent endeavors on the facile solution-phase synthesis of 1D and hollow inorganic nanostructures by chemical transformation from reactive templates.

*Corresponding author (email: liminqi@pku.edu.cn)

2 Synthesis of 1D nanostructures

For many kinds of inorganic materials, it is rather difficult to directly fabricate their 1D nanostructures at relatively low temperatures. To circumvent this obstacle, 1D reactive sacrificial templates can be utilized to fabricate 1D inorganic nanostructures with preserved 1D morphologies and desirable compositions through chemical transformation in solution, which provides a straightforward and effective route to fabricate 1D inorganic nanostructures. For example, because of the high reactivity of selenium, trigonal selenium (t-Se) nanowires have been demonstrated to be an effective sacrificial template for the fabrication of a variety of 1D metal chalcogenide nanostructures [30]. Xia *et al*. have synthesized Ag_2Se nanowires [31], CdSe nanotubes [32], and Pt nanotubes [33] by templating against t-Se nanowires. Long CdTe nanotubes with tunable diameters were synthesized by using diameter-tunable nanowires formed from Cd-TGA coordination polymers and PAA as the 1D sacrificial templates [34]. In a similar way, Zhu *et al*. reported a novel biomolecule-assisted route to the synthesis of lead chalcogenide polycrystalline nanotubes by templating against precursor nanowires composed of cysteine biomolecules, lead nitrate, and certain amines or ammonia [35]. In these reports, either ion exchange [34, 35] or redox [31, 32] reactions were utilized to obtain 1D nanostructures of target substances.

We synthesized nanofiber bundles of Ag_2S, Ag_2Se, and Ag by utilizing $Ag_2C_2O_4$ template nanofiber bundles through both anion-exchange and redox reactions [36]. A typical scanning electron microscopy (SEM) image of $Ag_2C_2O_4$ nanofiber bundles is displayed in Figure 1(a). Figures 1(b)–(d) show the transmission electron microscopy (TEM) images of the obtained Ag_2S, Ag_2Se, and Ag products. These bundles were all polycrystalline nanofibers composed of nanoparticles and the precursor morphology was well-preserved, indicating that $Ag_2C_2O_4$ nanofiber bundles acted as a general sacrificial template for the synthesis of silver-based semiconductor and metal nanofibers. In addition, an electrical transportation and switching device was built with the synthesized nanofiber bundles of Ag_2S and Ag, showing potential applications in nanoscale device building and integration.

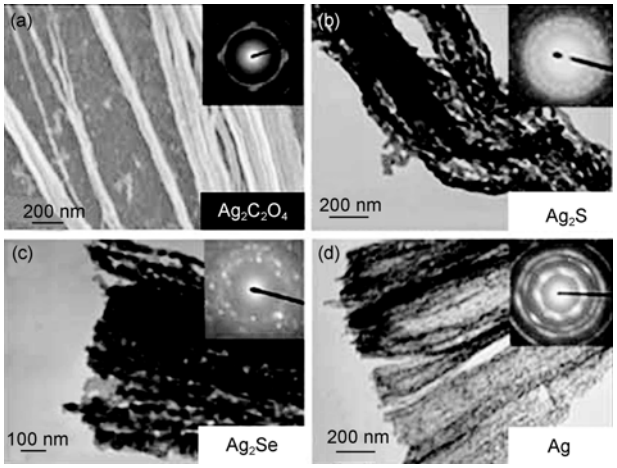

Figure 1 (a) An SEM image of $Ag_2C_2O_4$ nanofiber bundles. (b)–(d) TEM images of Ag_2S (b), Ag_2Se (c) and Ag (d) nanofiber bundles obtained by templating $Ag_2C_2O_4$ nanofibers. Insets show the corresponding ED patterns. Adapted from ref. [36].

Furthermore, we developed a facile and effective method to realize the transformation from t-Se nanotubes to PbSe nanotubes [37]. As shown in Figure 2, PbSe nanotubes with pseudo-hexagonal cross-sections were prepared by solvothermal transformation of well-faceted t-Se nanotubes in the presence of $Pb(Ac)_2$ and ascorbic acid in ethylene glycol at 200 °C. Moreover, novel Se@PbSe composite nanotubes consisting of Se nanotubes covered with a PbSe sheath were obtained by shortening the reaction time. Subsequent removal of the inner Se nanotubes resulted in the formation of thin-walled PbSe nanotubes (less than 20 nm in wall thickness). Preliminary electrochemical measurements showed that the prepared PbSe nanotubes exhibited a good electrochemical activity.

The controlled synthesis of 1D nanostructures and guiding them to ordered superstructures or complex functional architectures would offer great opportunities for exploring their novel properties and fabricating useful nanodevices [1, 3]. In this regard, it remains a great challenge to develop rational synthetic methods to fabricate complex nanorod/nanowire superstructures with desired architectures. We developed a novel 2D-template-engaged topotactic reaction method to synthesize hierarchical disc-like Bi_2S_3 networks composed of perpendicularly aligned single-crystalline nanorods [38]. Figure 3 shows typical SEM images of the BiOCl precursor discs obtained by the hydrolysis of $BiCl_3$ and the Bi_2S_3 networks obtained after reacting the BiOCl precursor discs with TAA. It was revealed that these superstructures were formed by the preferential growth of [001]-oriented Bi_2S_3 nanorods on the top faces of (001)-oriented BiOCl discs along the two perpendicular [100] and [010] directions of BiOCl. The measurements of the electrochemical hydrogen storage behaviors showed that the disc-like Bi_2S_3 nanorod networks could electrochemically charge and discharge with a capacity of 162 mA h g^{-1} at

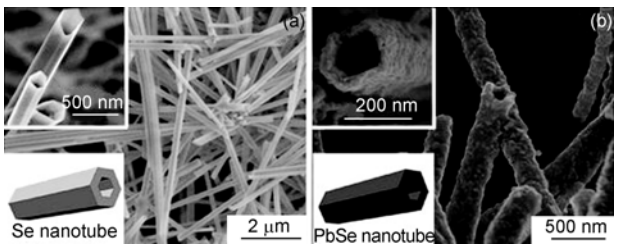

Figure 2 SEM images of Se nanotubes (a) and PbSe nanotubes (b). Insets show the mouths of the Se nanotubes (a) and PbSe nanotubes (b). Adapted from ref. [37].

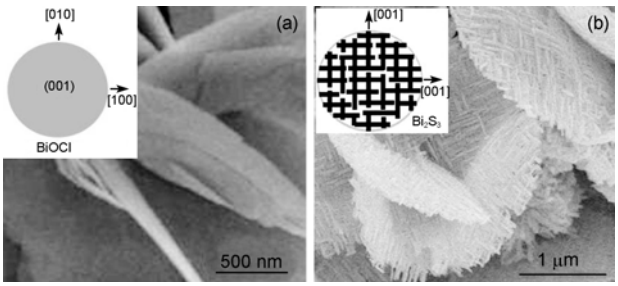

Figure 3 SEM images of BiOCl discs (a) and disc-like Bi_2S_3 nanorod networks (b) obtained by templating BiOCl discs. Insets show the schematic illustrations of the crystal orientation showing the topotactic transformation from the BiOCl disc to the Bi_2S_3 disc-like network. Adapted from ref. [38].

room temperature, indicating their potential applications in hydrogen storage, high-energy batteries, and catalytic fields.

The structural relationship between the *c*-axis of orthorhombic Bi_2S_3 ($c = 3.98$ Å) and the *a*- or *b*-axis of tetragonal BiOCl ($a = b = 3.89$ Å) could be responsible for the topotactic transformation from a single-crystalline disc-like template to a disc-like nanorod networks (Figure 4). When the sulfur ions released from TAA diffused to the top surfaces of BiOCl single-crystalline discs with the top faces of the (001) plane, the sulfur ions might replace the oxygen ions and chlorine ions to generate [001]-oriented Bi_2S_3 single-crystalline nanorods lying on the top surfaces due to lower solubility of Bi_2S_3. Moreover, these [001]-oriented Bi_2S_3

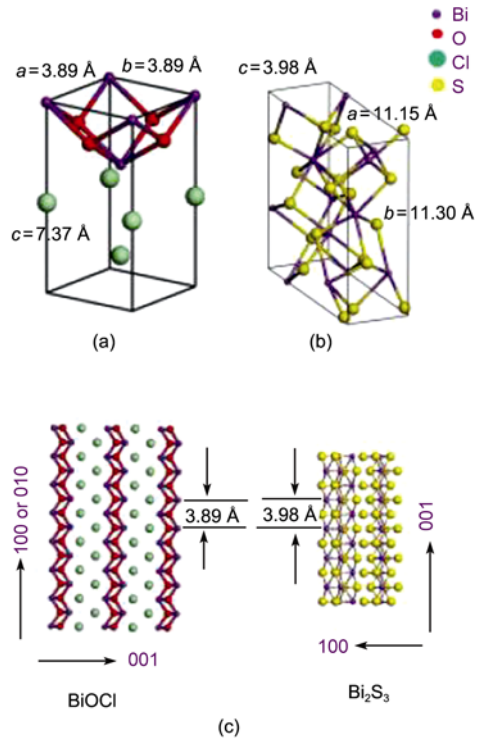

Figure 4 Schematic illustration of (a) the tetragonal BiOCl unit cell, (b) the orthorhombic Bi_2S_3 unit cell, and (c) the crystal lattice matching between tetragonal BiOCl and orthorhombic Bi_2S_3. Adapted from ref. [38].

single-crystalline nanorods tended to orient along the two perpendicular [100] and [010] directions of BiOCl due to the close lattice matching between the *c*-axis of Bi_2S_3 and the *a*- or *b*-axis of BiOCl, leading to the formation of a layer of disc-like network consisting of crossed nanorods on the top faces of BiOCl discs. The close lattice matching indicates a minimal reorganization of structure in the precursor solid, which could be the key to the formation of single-crystalline products from a single-crystalline template [30, 31]. The lattice constant of the *a*- or *b*-axis of BiOCl was essentially unchanged during the formation of [001]-oriented Bi_2S_3 single-crystalline nanorods upon topotactic transformation from the 2D precursor template. To the best of our knowledge, this work represents the first topotactic transformation process capable of generating 2D networks consisting of single-crystalline nanorods. This approach is potentially extendable to the fabrication of 2D networks made of 1D single-crystalline nanostructures with desirable properties and could open new avenues for the bottom-up fabrication of nanodevices assembled from 1D nanostructures.

3 Synthesis of hollow nanostructures

The synthesis via reactive templates has remarkable advantages in the large-yield preparation of hollow structures with designed sizes, nonspherical shapes, and hierarchical architectures [4, 8, 11]. These chemical processes include Kirkendall effect, galvanic replacement, oxidative evacuation, etc. Among them, the sacrificial template-directed chemical transformation method based on the Kirkendall effect has been demonstrated to be an effective approach [11, 29, 39, 40]. The Kirkendall effect is the mutual diffusion rates of two components in a diffusion couple differ by a considerable amount so that vacancy diffusion occurs to compensate for the inequality of the material flow and the initial interface moves [41, 42]. The physical phenomenon may provide possibilities for fabrication of new nanomaterials with hollow interiors considering the directional matter flow and consequential vacancy accumulation in Kirkendall type diffusion. In this part, we focus on the work done in our lab on the synthesis of hollow structures based on the Kirkendall effect.

We prepared uniform copper sulfide and oxide hollow spheres by using reactive templates based on the Kirkendall effect [43]. The *in situ* formed sacrificial template containing Cu(I) can be employed as a general reactive template for the fabrication of hollow microspheres of Cu_2O and Cu_xS. The shell thickness of these hollow spheres can be adjusted through the choice of the bromide source used for the formation of intermediate templates. As shown in Figures 5(a) and (b), thick-shell CuS hollow spheres with a shell thickness of about 130–180 nm were obtained by using CuBr solid spheres as the templates, which were formed by the

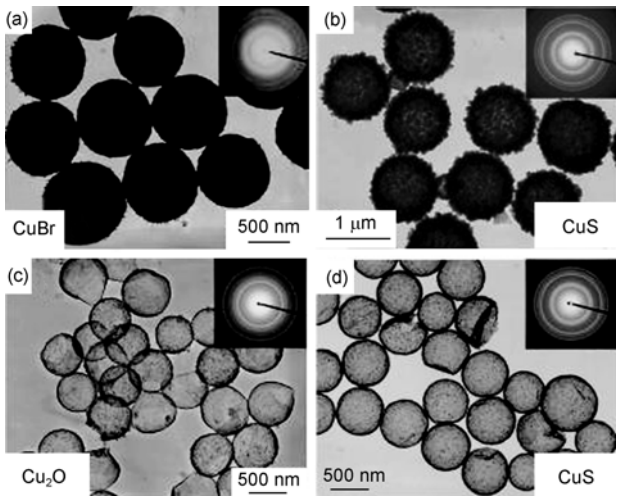

Figure 5 TEM images of (a) CuBr spheres, (b) thick-shell CuS hollow spheres, (c) thin-shell Cu_2O hollow spheres, and (d) thin-shell CuS hollow spheres. Insets show the corresponding ED patterns. Adapted from ref. [43].

reduction of $CuBr_2$ with ascorbic acid. Uniform thin-shell hollow spheres of Cu_2O and CuS with a shell thickness of about 20–25 nm (Figures 5(c) and (d)) can be readily obtained if Cu(I)–containing aggregates instead of CuBr solid spheres are employed as the template. In this case, $(C_4H_9)_4NBr$ and $CuCl_2$ were respectively used as the bromide and copper sources, rather than the use of $CuBr_2$ as both the bromide and copper sources. The shell thickness of the hollow spheres could be related to the content of Cu(I) ions in the spherical templates. A relatively smaller content of Cu(I) ions in the loose aggregates would result in a much thinner shell for the final hollow spheres. It was also revealed that these Cu_2O and CuS hollow spheres exhibited remarkable optical limiting effects, making them useful for protecting human eyes or optical sensors from high-power laser irradiation. In a similar way, we synthesized hierarchical, core-shell structured microspheres of a series of bismuth chalcogenides by chemical transformation of intermediate BiOCl microspheres [44]. Dong and co-workers developed a facile and general method for the rapid synthesis of hollow urchinlike metallic or bimetallic nanostructures by using in-situ produced Ag nanoparticles as sacrificial templates [45]. Xie *et al*. reported a novel and convenient synthetic route to VOOH double-shelled hollow spheres from the $V(OH)_2NH_2$ solid templates via programming the reaction-temperature procedures [46].

The reactive templates can be extended to the synthesis of nonspherical hollow structures. In particular, we obtained hierarchical assembly of rhombododecahedral silver cages through the microscale Kirkendall effect by employing rhombododecahedral Ag_3PO_4 crystals as reactive precursor templates [47]. As shown in Figure 6(a), Ag_3PO_4 crystals with uniform rhombododecahedral morphology were used as the precursor for the morphology-preserved synthesis of silver particles using different reducing agents. Figure 6(b) shows the SEM image of single-walled Ag rhombododecahedral cages obtained by the reduction of the precursor crystals in ascorbic acid solution. It suggests the formation of hollow silver particles with a well preserved rhombododecahedral morphology. Hydrazine is a stronger reductant and has a higher diffusion ability than ascorbic acid, and unique double-walled Ag cages with rhombododecahedral morphology can be obtained when hydrazine is used as the reductant instead of ascorbic acid (Figure 6(c)). The double-walled pattern is reminiscent of the well-known Liesegang patterns [48] which typically form by a periodic precipitation through the moving reaction front when two coprecipitating reactants interdiffuse in a gel medium. When $NaBH_4$, which has an even higher reducing ability and diffusion ability, was used as the reducing agent, novel core–shell structured silver rhombododecahedra were produced (Figure 6(d)).

A tentative mechanism was proposed for the formation of the three different types of silver rhombododecahedra (Figure 7). Briefly, a layer of interconnected silver networks forms around the exterior surface of the Ag_3PO_4 rhombododecahedra as long as they are surrounded by a sufficient concentration of the reductant. Then, the network layer develops into a denser shell, which is accompanied by the formation of a depletion layer near the shell as a result of the coupled reaction/diffusion process. The final silver structure depends on the inward diffusion rate of the reductant relative to the outward diffusion rate of the Ag^+ ions, i.e., single-walled rhombododecahedra form with ascorbic acid, which has a low diffusion rate, whereas double-walled rhombododecahedra form with hydrazine, which has a medium diffusion rate, and core–shell structured rhombodo-

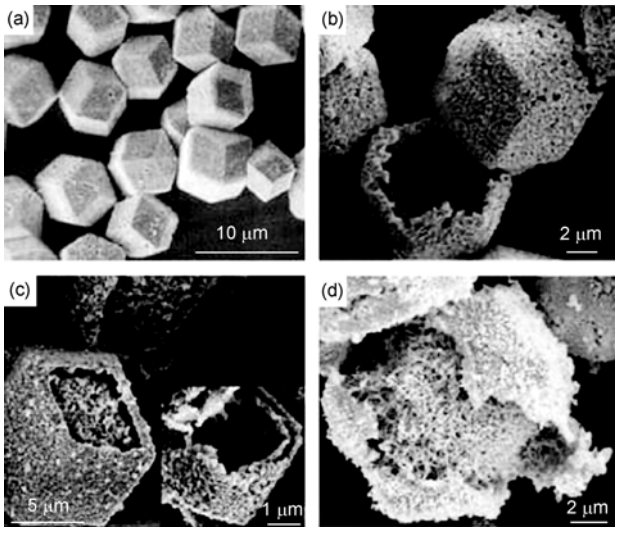

Figure 6 SEM images of (a) Ag_3PO_4 rhombododecahedral crystals and (b)–(d) silver rhombododecahedral particles obtained using different reducing agents: (b) single-walled cages produced with ascorbic acid, (c) double-walled cages produced with hydrazine, and (d) core-shell structured particles produced with $NaBH_4$. Adapted from ref. [47].

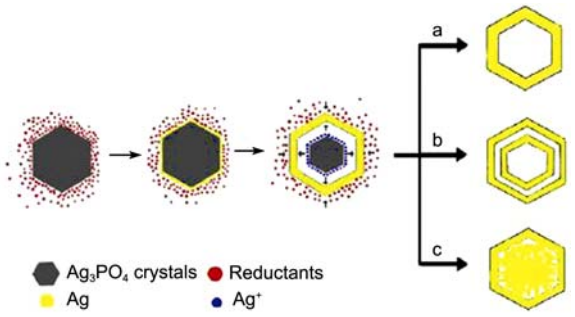

Figure 7 Schematic illustration of the formation of hierarchical, silver rhombododecahedral particles: (a) single-walled cages, (b) double-walled cages, and (c) core–shell structured particles. Reprinted from ref. [47].

decahedra form with $NaBH_4$, which has a high diffusion rate. The controlled self-assembly of silver particles produced *in situ* around the precursor crystal surfaces can lead to the formation of morphology-preserved, single- or double-walled silver cages constructed from different building units, such as particles, nanoplates, and quasispherical assemblies of nanoplates. This process provides a general route to the synthesis of silver superstructures with unique morphologies and complex hierarchies. Furthermore, this strategy may be extended to other metal systems and could possibly be used for device fabrication with appropriate metal/precursor/reductant combinations.

Another example for the synthesis of non-spherical hollow structure through reactive templates is the fabrication of octahedral Cu_2O nanocages by a catalytic solution route, which involves the formation of octahedral Cu_2O nanocrystals and a subsequent spontaneous hollowing process through oxidative evacuation [49]. In this synthesis, $PdCl_2$ was introduced into the reaction mixture of Fehling's solution (copper–tartrate complex) and the reductant glucose for the catalytic solution synthesis of unique octahedral Cu_2O nanocages. Typical SEM and TEM images of the Cu_2O crystals obtained after 3 h of aging are shown in Figure 8, which suggest that the product exhibits uniform, regular octahedral nanocages with a wall thickness typically in the 10–14 nm range. What is more, a wealth of colorful Cu_2O nanostructures with widely tunable bandgaps in the range of 2.6–2.2 eV have been obtained by this synthetic route. This facile one-pot approach to inorganic hollow structures with

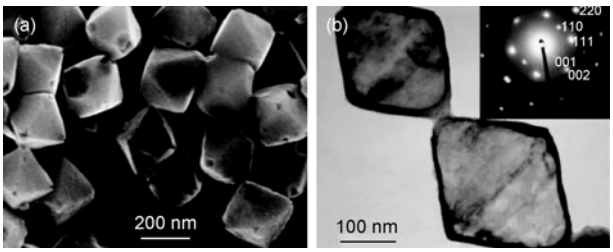

Figure 8 SEM (a) and TEM (b) images of octahedral Cu_2O nanocages obtained by a catalytic etching route. The inset to (b) shows the SAED pattern of the upper Cu_2O nanocage. Adapted from ref. [49].

novel morphologies could be potentially extended to other inorganic systems.

Based on the examination of the time-dependent formation of octahedral Cu_2O nanocages, it was proposed that the octahedral nanocages are formed by a two-step process, i.e., the formation of octahedral solid nanocrystals by the Pd-catalyzed reduction of the copper–tartrate complex with glucose, and the subsequent hollowing of the nanooctahedra due to a Pd-catalyzed, oxygen-engaged oxidation process. During the first step, $PdCl_2$ may be reduced to small Pd^0 nanoparticles by glucose prior to the reduction of Cu^{2+}–tartrate complex and then Pd acts as a catalyst for the reductive transformation of Cu^{2+} to Cu_2O particles, similar to the electroless copper plating process activated by $PdCl_2$. During the second step, the trace oxygen dissolved in the solution may gradually oxidize Cu_2O into Cu^{2+} in the presence of the Pd catalyst. The Pd catalyst could play an important role in the selective etching of the octahedral apexes and the preferential evacuation of the octahedra. Since the adsorption of tartrate ions on the surfaces of the octahedra could considerably prevent the direct contact of the Pd catalyst, the preferential oxidative etching of the apexes of the Cu_2O octahedra would occur due to their relatively higher activity. Subsequently, dissolved oxygen together with the Pd catalyst would continue to diffuse into the interior through the open corners, resulting in a gradual hollowing of the octahedra.

Several other research groups from China have made great contributions to the fabrication of nonspherical hollow structures by using shape-controlled solid precursors as reactive templates. For example, Qian and co-workers synthesized highly symmetric 18-facet polyhedron nanocrystals of Cu_7S_4 with a hollow nanocage through the chemical transformation of truncated cubic Cu_2O nanocrystals [50]. Xu *et al*. prepared well-defined non-spherical copper sulfide mesocages with single-crystalline shells by shape-controlled Cu_2O crystal templating [51]. Xie *et al*. synthesized micrometer scaled MoS_2 hierarchical hollow cubic cages assembled by bilayers via a one-step self-assembly coupled with intermediate crystal templating process, in which the intermediate $K_2NaMoO_3F_3$ crystal formed in-situ and then served as the self-sacrificed template based on the Kirkendall effect [52]. Li *et al*. reported the synthesis of hierarchical hollow MnO_2 microcubes by shape-preserving oxidation of $MnCO_3$ microcubes [53]. Recently, Yu *et al*. described the hydrothermal synthesis of novel anatase TiO_2 boxes by using rectangular particulates with a composition of $(TiO_2)_2{\cdot}C_4H_6O_5{\cdot}6H_2O$ as reactive templates [54].

4 Conclusions

In this paper, we summarized our recent research results on the solution-phase synthesis of inorganic nanostructures by chemical transformation from reactive templates. The sacri-

ficial template-directed chemical transformation strategy provides a simple and versatile route to fabricate both 1D and hollow nanostructures, and it is potentially extendable to the controlled synthesis of other kinds of inorganic nanostructures if suitable templates and reactions are employed.

In the past decade, significant progress has been made in the bottom-up fabrication of both 1D and hollow inorganic nanostructures. Among various synthetic strategies, solution-phase chemical transformation of reactive templates is advantageous in terms of cost, throughput, modulation of composition, and the potential for large-scale and environmentally benign production. A variety of 1D and hollow inorganic nanostructures with designed size, shape, composition and function have been prepared by employing reactive sacrificial templates. However, research on this strategy is still in its infancy and much work needs to be done in the following aspects: realization of the precise control over the composition, crystal structure, surface properties, and hierarchical assembly of inorganic nanostructures, detailed investigation on the formation mechanisms, and realization of the large-scale and environmentally benign synthesis in industries.

This work was supported by the National Natural Science Foundation of China (Grant Nos. 20873002, 20673007, 20633010, and 50821061), MOST (Grant No. 2007CB936201), and SRFDP (Grant No. 20070001018).

1 Xia YN, Yang PD, Sun YG, Wu YY, Mayers B, Gates B, Yin YD, Kim F, Yan HQ. One-dimensional nanostructures: synthesis, characterization, and applications. *Adv Mater*, 2003, 15: 353–389
2 Goldberger J, Fan R, Yang PD. Inorganic nanotubes: a novel platform for nanofluidics. *Acc Chem Res*, 2006, 39: 239–248
3 Lieber CM, Wang ZL. Functional nanowires. *MRS Bull*, 2007, 32: 99–108
4 Lou XW, Archer LA, Yang ZC. Hollow micro-/nanostructures: synthesis and applications. *Adv Mater*, 2008, 20: 3987–4019
5 Tong WJ, Gao CY. Multilayer microcapsules with tailored structures for bio-related applications. *J Mater Chem*, 2008, 18: 3799–3812
6 Skrabalak SE, Chen JY, Au L, Lu XM, Li XD, Xia YN. Gold nanocages for biomedical applications. *Adv Mater*, 2007, 19: 3177–3184
7 Ye JF, Qi LM. Solution-phase synthesis of one-dimensional semiconductor nanostructures. *J Mater Sci Technol*, 2008, 24: 529–540
8 Ma YR, Qi LM. Solution-phase synthesis of inorganic hollow structures by templating strategies. *J Colloid Interface Sci*, 2009, 335: 1–10
9 van Bommel KJC, Friggeri A, Shinkai S. Organic templates for the generation of inorganic materials. *Angew Chem Int Ed*, 2003, 42: 980–999
10 Hurst SJ, Payne EK, Qin LD, Mirkin CA. Multisegmented one-dimensional nanorods prepared by hard-template synthetic methods. *Angew Chem Int Ed*, 2006, 45: 2672–2692
11 Fan HJ, Gosele U, Zacharias M. Formation of nanotubes and hollow nanoparticles based on Kirkendall and diffusion processes: a review. *Small*, 2007, 3: 1660–1671
12 Wu YY, Livneh T, Zhang YX, Cheng GS, Wang JF, Tang J, Moskovits M, Stucky GD. Templated synthesis of highly ordered mesostructured nanowires and nanowire arrays. *Nano Lett*, 2004, 4: 2337–2342
13 Zhang DY, Yang D, Zhang HJ, Lu CH, Qi LM. Synthesis and photocatalytic properties of hollow microparticles of titania and titania/carbon composites templated by Sephadex G-100. *Chem Mater*, 2006, 18:3477–3485
14 Zhao NN, Wei Y, Sun NJ, Chen Q, Bai JW, Zhou LP, Qin Y, Li MX, Qi LM. Controlled synthesis of gold nanobelts and nanocombs in aqueous mixed surfactant solutions. *Langmuir*, 2008, 24: 991–998
15 Ma YR, Qi LM, Ma JM, Cheng HM. Micelle-mediated synthesis of single-crystalline selenium nanotubes. *Adv Mater*, 2004, 16: 1023–1026
16 Ma YR, Qi LM, Shen W, Ma JM. Selective synthesis of single-crystalline selenium nanobelts and nanowires in micellar solutions of nonionic surfactants. *Langmuir*, 2005, 21: 6161–6164
17 Zhang DB, Qi LM, Yang JH, Ma JM, Cheng HM, Huang L. Wet chemical synthesis of silver nanowire thin films at ambient temperature. *Chem Mater*, 2004, 16: 872–876
18 Bai JW, Qin Y, Jiang CY, Qi LM. Polymer-controlled synthesis of silver nanobelts and hierarchical nanocolumns. *Chem Mater*, 2007, 19: 3367–3369
19 Ma YR, Qi LM, Ma JM, Cheng HM. Facile synthesis of hollow ZnS nanospheres in block copolymer solutions. *Langmuir*, 2003, 19: 4040–4042
20 Ma YR, Qi LM, Ma JM, Cheng HM, Shen W. Synthesis of submicrometer-sized CdS hollow spheres in aqueous solutions of a triblock copolymer. *Langmuir*, 2003, 19: 9079–9085
21 Shi HT, Qi LM, Ma JM, Cheng HM. Polymer-directed synthesis of penniform $BaWO_4$ nanostructures in reverse micelles. *J Am Chem Soc*, 2003, 125: 3450–3451
22 Qi LM, Li J, Ma JM. Biomimetic morphogenesis of calcium carbonate in mixed solutions of surfactants and double-hydrophilic block copolymers. *Adv Mater*, 2002, 14: 300–303
23 Zhang DB, Qi LM, Ma JM, Cheng HM. Synthesis of submicrometer-sized hollow silver spheres in mixed polymer-surfactant solutions. *Adv Mater*, 2002, 14: 1499–1502
24 Li Z, Chung SW, Nam JM, Ginger DS, Mirkin CA. Living templates for the hierarchical assembly of gold nanoparticles. *Angew Chem Int Ed*, 2003, 42: 2306–2309
25 Chen CL, Zhang PJ, Rosi NL. A new peptide-based method for the design and synthesis of nanoparticle superstructures: construction of highly ordered gold nanoparticle double helices. *J Am Chem Soc*, 2008, 130: 13555–13557
26 Zhang HJ, Wu J, Zhou LP, Zhang DY, Qi LM. Facile synthesis of monodisperse microspheres and gigantic hollow shells of mesoporous silica in mixed water-ethanol solvents. *Langmuir*, 2007, 23: 1107–1113
27 Sun YG, Xia YN. Shape-controlled synthesis of gold and silver nanoparticles. *Science*, 2002, 298: 2176–2179
28 Son DH, Hughes SM, Yin YD, Alivisatos AP. Cation exchange reactions in ionic nanocrystals. *Science*, 2004, 306: 1009–1012
29 Yin YD, Rioux RM, Erdonmez CK, Hughes S, Somorjai GA, Alivisatos AP. Formation of hollow nanocrystals through the nanoscale kirkendall effect. *Science*, 2004, 304: 711–714
30 Jeong U, Camargo PHC, Lee YH, Xia YN. Chemical transformation: a powerful route to metal chalcogenide nanowires. *J Mater Chem*, 2006,16: 3893–3897
31 Gates B, Wu YY, Yin YD, Yang PD, Xia YN. Single-crystalline nanowires of Ag_2Se can be synthesized by templating against nanowires of trigonal Se. *J Am Chem Soc*, 2001, 123: 11500–11501
32 Jiang XC, Mayers B, Herricks T, Xia YN. Direct synthesis of Se@CdSe nanocables and CdSe nanotubes by reacting cadmium salts with Se nanowires. *Adv Mater*, 2003, 15: 1740–1743
33 Mayers B, Jiang XC, Sunderland D, Cattle B, Xia YN. Hollow nanostructures of platinum with controllable dimensions can be synthesized by templating against selenium nanowires and colloids. *J Am Chem Soc*, 2003, 125: 13364–13365
34 Niu HJ, Gao MY. Diameter-tunable CdTe nanotubes templated by 1D nanowires of cadmium thiolate polymer. *Angew Chem Int Ed*, 2006, 45: 6462–6466
35 Tong H, Zhu YJ, Yang LX, Li L, Zhang L. Lead chalcogenide nano-

tubes synthesized by biomolecule-assisted self-assembly of nanocrystals at room temperature. *Angew Chem Int Ed*, 2006, 45: 7739–7742
36 Wang HL, Qi LM. Controlled synthesis of Ag_2S, Ag_2Se and Ag nanofibers using a general sacrificial template and their application in electronic device fabrication. *Adv Funct Mater*, 2008, 18: 1249–1256
37 Huang T, Qi LM. Controlled Synthesis of PbSe nanotubes by solvothermal transformation from selenium nanotubes. *Nanotechnology*, 2009, 20: 025606
38 Li LS, Sun NJ, Huang YY, Qin Y, Zhao NN, Gao JN, Li MX, Zhou HH, Qi LM. Topotactic transformation of single-crystalline precursor discs into disc-like Bi_2S_3 nanorod networks. *Adv Funct Mater*, 2008, 18: 1194–1201
39 Zeng HC. Synthetic architecture of interior space for inorganic nanostructures. *J Mater Chem*, 2006, 16: 649–662
40 Fan HJ, Knez M, Scholz R, Hesse D, Nielsch K, Zacharias M, Gosele U. Influence of surface diffusion on the formation of hollow nanostructures induced by the Kirkendall effect: the basic concept. *Nano Lett*, 2007, 7: 993–997
41 Smigelskas AD, Kirkendall EO. Zinc diffusion in alpha brass. *Trans AIME*, 1947, 171: 130–142
42 Kirkendall EO. Diffusion of zinc in alpha brass. *Trans AIME*, 1942, 147: 104–110
43 Gao JN, Li QS, Zhao HB, Li LS, Liu CL, Gong QH, Qi LM. One-pot synthesis of uniform Cu_2O and CuS hollow spheres and their optical limiting properties. *Chem Mater*, 2008, 20: 6263–6269
44 Li LS, Cao RG, Wang ZJ, Li JJ, Qi LM. Template synthesis of hierarchical Bi_2E_3 (E = S, Se, Te) core-shell microspheres and their electrochemical and photoresponsive properties. *J Phys Chem C*, 2009, 113: 18075–18081
45 Guo SJ, Dong SJ, Wang EK. A general method for the rapid synthesis of hollow metallic or bimetallic nanoelectrocatalysts with urchinlike morphology. *Chem Eur J*, 2008, 14: 4689–4695
46 Wu CZ, Zhang XD, Ning B, Yang JL, Xie Y. Shape evolution of new-phased lepidocrocite VOOH from single-shelled to double-shelled hollow nanospheres on the basis of programmed reaction-temperature strategy. *Inorg Chem*, 2009, 48: 6044–6054
47 Yang JH, Qi LM, Lu CH, Ma JM, Cheng HM. Morphosynthesis of rhombdodecahedral silver cages by self-assembly coupled with precursor crystal templating. *Angew Chem Int Ed*, 2005, 44: 598–603
48 Liesegang RE. Ueber einige eigenschaften von gallerten. *Naturwissenschaften*, 1896, 11: 353–362
49 Lu CH, Qi LM, Yang JH, Wang XY, Zhang DY, Xie JL, Ma JM. One-pot synthesis of octahedral Cu_2O nanocages by a catalytic solution route. *Adv Mater*, 2005, 17: 2562–2567
50 Cao HL, Qian XF, Wang C, Ma XD, Yin J, Zhu ZK. High symmetric 18-facet polyhedron nanocrystals of Cu_7S_4 with a hollow nanocage. *J Am Chem Soc*, 2005, 127: 16024–16025
51 Jiao SH, Xu LF, Jiang K, Xu DS. Well-defined non-spherical copper sulfide mesocages with single-crystalline shells by shape-controlled Cu_2O crystal templating. *Adv Mater*, 2006, 18: 1174–1177
52 Ye LN, Wu CZ, Guo W, Xie Y. MoS_2 hierarchical hollow cubic cages assembled by bilayers: one-step synthesis and their electrochemical hydrogen storage properties. *Chem Commun*, 2006, 4738–4740
53 Fei JB, Cui Y, Yan XH, Qi W, Yang Y, Wang KW, He Q, Li JB. Controlled preparation of MnO_2 hierarchical hollow nanostructures and their application in water treatment. *Adv Mater*, 2008, 20: 452–456
54 Liu SJ, Wu XX, Hu B, Gong JY, Yu SH. Novel anatase TiO_2 boxes and tree-like structures assembled by hollow tubes: D,L-malic acid-assisted hydrothermal synthesis, growth mechanism, and photocatalytic properties. *Cryst Growth Des*, 2009, 9: 1511–1518